

Experimental evidence of the decoupling line in $(\text{Bi}_{1.64}\text{Pb}_{0.36})\text{Sr}_2(\text{Ca}_{0.79}\text{Y}_{0.21})\text{Cu}_2\text{O}_{8+\delta}$ single crystals by resistivity measurements

D. Thopart, Ch. Goupil, and Ch. Simon

Laboratoire CRISMAT, UMR 6508, CNRS, ISMRA et Université de Caen, 6 Bd du Maréchal Juin, 14050 Caen-Cedex, France

(Received 20 October 2000; revised manuscript received 30 January 2001; published 4 April 2001)

Both in-plane (ρ_{ab}) and out-of-plane (ρ_c) resistivity measurements have been carried out on $(\text{Bi}_{1.64}\text{Pb}_{0.36})\text{Sr}_2(\text{Ca}_{0.79}\text{Y}_{0.21})\text{Cu}_2\text{O}_{8+\delta}$ single crystals with magnetic field applied along the c -axis direction. Studying the temperature dependence of the resistivity ratio ρ_{ab}/ρ_c , we identify at high temperature a pancake phase with the signature proposed by Koshelev. At lower temperature, we observe a thermally activated behavior which can be interpreted easily in the framework of a three-dimensional vortex loops model. We found that the high-temperature limit of the thermally activated behavior corresponds to the low-temperature limit of the Koshelev's prediction. This latter is also characterized by an onset of the in-plane resistivity drop. Consequently, our data suggest that this line is a dimensional crossover which describes the decoupling of the liquid state into a decoupled pancake state.

DOI: 10.1103/PhysRevB.63.184504

PACS number(s): 74.60.Ec, 74.25.Fy, 74.72.Hs

I. INTRODUCTION

It is generally well established that the sharp drop of resistivity observed in the mixed state is the result of a first order transition of the vortex lattice. It may correspond either to a melting transition¹⁻⁴ or to a decoupling one.⁵ However, the first order transition is very sensitive to the state of disorder⁶⁻⁸ and should lead to a second order transition when increasing the disorder. In this case, a drop of resistivity should correspond to a second order transition or a continuous crossover in the vortex diagram. On the other hand, if one assumes this drop to be a change of dimensionality of the vortices (decoupling transition or crossover), the three-dimensional (3D) and 2D behaviors should be observable. Moreover, in a “field/temperature” diagram, this crossover line should decrease as the anisotropy increases.⁹⁻¹¹

In a highly anisotropic compounds such as Bi-2212, the theoretical analysis in terms of activation energies at low temperature revealed that the field dependence of these energies was proportional to $(B^{-1/2})^{12-16}$ in the case of 3D vortices. Increasing the temperature, the application of these models should not be anymore valid, due to the pancakes decoupling, driving the 3D vortex lattice into a 2D system at high temperature.^{17,18} Above this decoupling line, the system can be regarded as sets of 2D vortices independent from a layer to another. On these considerations, Koshelev¹⁸ proposed a description of this 2D vortex state where the c -axis resistivity ρ_c should be related to the measured ρ_{ab} . In 1992, Busch *et al.*¹⁹ have measured in Bi-2212 the in and out of plane resistivities in a single crystal by a six-terminal method. But this method made several approximations which are not always fulfilled in the present case, as we have shown by a more exact numerical calculation.²⁰

Consequently, in order to describe the dimensionality of the vortices on the whole (B, T) phase diagram, several theoretical approach are needed since none of them is able to describe all the underlying mechanisms of dissipation. The aim of this paper is to identify, on the same sample and by a different experimental technique, the 3D and 2D characters

of the vortices and analyze them using various models and determine the limits of validity of them.

II. EXPERIMENT

The single crystals of $(\text{Bi}_{1.64}\text{Pb}_{0.36})\text{Sr}_2(\text{Ca}_{0.79}\text{Y}_{0.21})\text{Cu}_2\text{O}_{8+\delta}$ are grown by a self-flux method. The details of the growth are reported elsewhere.^{21,22} The results presented here are typical of all the samples of the same batch. The dimensions of the crystal that we have chosen to present here are $960 \mu\text{m} \times 820 \mu\text{m} \times 20 \mu\text{m}$ with the lower dimension parallel to the c -axis direction. We have evaporated six “silver pads” as described in Fig. 1. These pads cross the whole width of the crystals. Two of them on the top face, two others on the bottom face and one “silver pad” on each ac face. With this simple contacts configuration, we measured the in-plane ρ_{ab} and the out-of-plane ρ_c resistivities on the same crystal. Indeed, the measurement of the ρ_c resistivity needs to apply the current along the c -axis direction and measure the voltage drop parallel to it. This simple contacts configuration leads to a good estimate of ρ_c , as discussed by Hardy *et al.*^{23,20} for Bi-2212 single crystals. On the other hand, for the in-plane resistivity measurement, the current is applied within the ab plane, i.e., between the two ac planes, and the voltage drop is measured with either the two contacts on the top face or the two others of the bottom face. On Fig. 1, we report the two different contacts configurations used in this study. All the measurements were performed in the linear regime ($I = 1 \text{ mA}$), in which the critical current was checked to be zero. This rules out any possible effect of geometrical barriers, previously

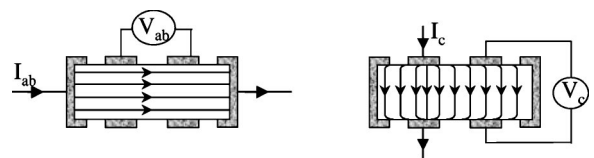


FIG. 1. The in-plane (left side) and out-of-plane (right side) contacts configurations.

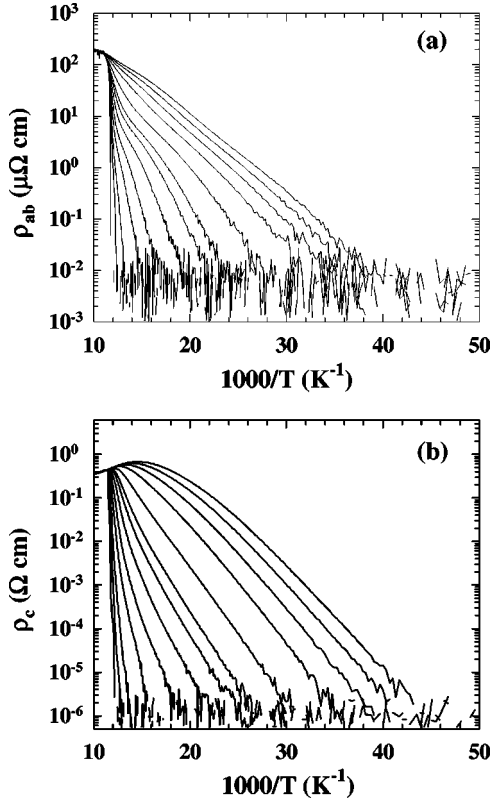


FIG. 2. Temperature dependence of the in-plane (a) and out-of-plane (b) resistivities in the Arrhenius plot for magnetic fields $B\parallel c$ of $B=0, 0.01, 0.02, 0.05, 0.1, 0.2, 0.35, 0.5, 1, 2, 3, 4, 5$ T from the left to the right. The injected current is 1 mA for both cases.

reported in similar samples in the solid phase at low magnetic field.²⁴

In order to reduce the contact resistances, we annealed the sample at $T=400$ °C during ten minutes. After annealing, the contact resistances are close to $1\ \Omega$.

The resistivity measurements were performed by a Physical Property Measurement System (PPMS model 6000 from quantum design) with decreasing temperature and an applied magnetic field up to 5 T. The ac susceptibility measurements were performed by a SQUID susceptometry with a fixed magnetic field and temperature and with a frequency varying from 10^{-1} to 10^3 Hz.

III. RESULTS AND DISCUSSION

In Fig. 2, we report the in-plane and out-of-plane resistivity measurements under magnetic field parallel to the c axis. The critical temperature is $T_c=86$ K with a transition width $\Delta T_c\sim 2$ K as determined by a SQUID dc magnetization measurement under 1 G. Moreover, at room temperature, $\rho_{ab}=300\ \mu\Omega\text{ cm}$ and $\rho_c=0.25\ \Omega\text{ cm}$. These values are in good agreement with previous reports.^{23,25–27}

In the normal state, the in-plane resistivity presents a linear temperature dependence while the c -axis resistivity shows a ‘‘semiconductinglike’’ behavior. On the other hand, in the superconducting state, the ρ_{ab} curves present two different behaviors: at higher field, the ρ_{ab} resistivity decreases

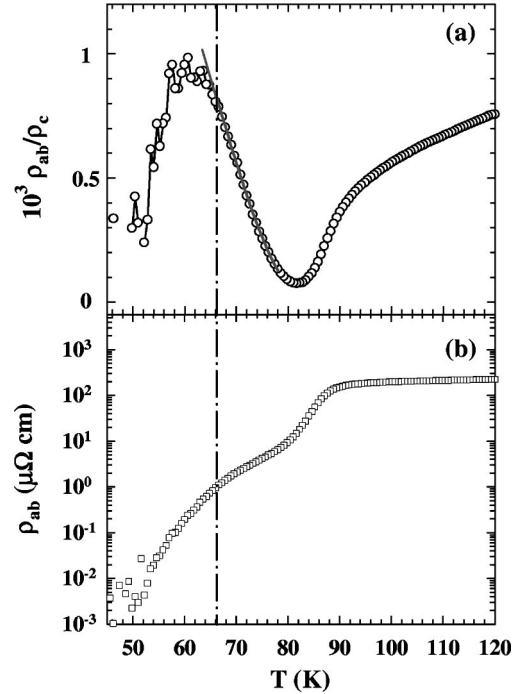


FIG. 3. Temperature dependence of the resistivity ratio ρ_{ab}/ρ_c (a) and in-plane resistivity (b) for a $B=0.2$ T magnetic field applied parallel to the c -axis direction. The solid line (a) corresponds to the fit expression proposed by Koshelev. The dash-dotted line represents the low temperature limit of the 2D model proposed by Koshelev.

rather smoothly with the temperature and no anomaly is observed while at lower field, a shoulder is observed in the low temperature end of the ρ_{ab} curves. For the c -axis resistivity measurements, the same characteristic curves can be seen but the shoulder is less pronounced than in the in-plane resistivity case. Consequently, the in-plane and out-of-plane resistivities present roughly a similar temperature dependence.

From a theoretical point of view, one expects that for field larger than the crossover field $B_{cr}=\phi_0/(\gamma d)^2=0.1$ T and temperature larger than the decoupling temperature T_{dec} , the vortex system can be analyzed as a set of independent two-dimensional vortex lattice in the layers.¹⁷ Here ϕ_0 is the flux quantum, γ is the anisotropy ratio, and d is half the interlayer spacing. The in-plane dissipation is then due to the thermally activated motion of mobile pancake vortices. The c -axis conductivity is of Josephson origin and is caused by the phase slips between neighboring pancakes in adjacent CuO_2 layers. In the Koshelev model,¹⁸ describing the decoupled 2D pancakes phase, the author finds a relation between ρ_c and ρ_{ab} . Koshelev supposes that the phase slips are caused by the diffusive motion of the small amount of pancake vortices independently in the different layers. In order to verify the theoretical Koshelev’s prediction, we have plotted on Fig. 3 the temperature dependence of the $\rho_{ab}/\rho_c(T,B)$ ratio for a $B=0.2$ T magnetic field. In Fig. 4, for all the magnetic field between $B=0$ and $B=5$ T, the temperature dependence of the $\rho_{ab}/\rho_c(T,B)$ ratio are illustrated. The curves are then fitted using the temperature dependence $\rho_{ab}/\rho_c(T,B)=A(B)[(1-T/T_c)^2/\rho_{cn}^2 T^2]$ as proposed by Koshelev.¹⁸ In this expression, A is the fitting parameter and ρ_{cn} is the nor-

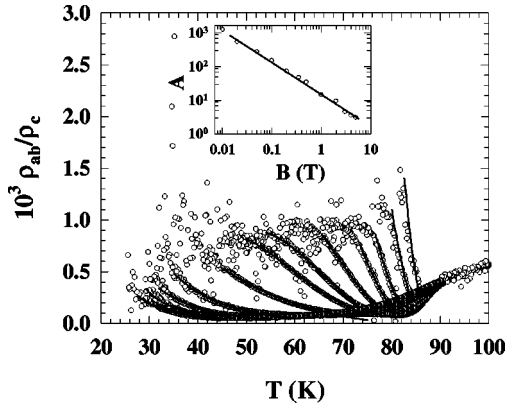


FIG. 4. Temperature dependence of the resistivity ratio ρ_{ab}/ρ_c for various magnetic field applied parallel to the c -axis direction. The applied magnetic field is to $B=0.01, 0.02, 0.05, 0.1, 0.2, 0.35, 0.5, 1, 2, 3, 4, 5$ T. The solid lines correspond to the fit expression proposed by Koshelev. In the inset, the field dependence of the fitting parameter A is plotted where the solid line corresponds to a B^{-1} dependence.

mal state c -axis resistivity. We have used the phenomenological expression proposed by Yan *et al.*²⁸ where $\rho_{cn}(T) = \rho_0 + bT + (c/T)\exp(\Delta/T)$ with $\rho_0 \approx 0.20 \Omega \text{ cm}$, $b \approx 1.43 \times 10^{-4} \Omega \text{ cm K}^{-1}$, $c \approx 1.45 \Omega \text{ cm K}$, $\Delta \approx 233.9 \text{ K}$. Let us note the magnetic field dependence of the fitting parameter $A(B)$. According to the Koshelev's model, the fitting parameter should be proportional to the inverse of the magnetic field: $A(B) \propto 1/B$.

In Figs. 3(a) and 4, we observe that the theoretical expression described above fit perfectly our data. On these figures, the fits are represented by the solid lines. The magnetic field dependence of the fitting parameter is also in perfect agreement with the theory as illustrated in the inset of the Fig. 4 where the solid line corresponds to a B^{-1} dependence. Nevertheless, we can observe that our data are not well fitted at low temperature as shown in Fig. 3(a). Consequently, in the high-temperature part of the $\rho_{ab}(T, B)$ curves, the ‘‘vortex matter’’ seems to correspond with a decoupled pancakes. Recently, Chung *et al.*²⁹ identified this 2D vortex state using the Koshelev expression. For lower magnetic field, the low-temperature limit of the model (this limit is marked by a dash-dotted line on Fig. 3 for $B=0.2$ T) corresponds roughly to the temperature drop of ρ_{ab} described above by a shoulder as shown in Fig. 3. In Fig. 7, we plotted this limit by a solid line. This latter represents a decoupling crossover.

It has been observed that the low-temperature part of the resistivity curves is consistent with a thermally activated dissipation mechanism.^{16,30–32} From the Fig. 2, at lower temperature, the in-plane resistivity present an Arrhenius behavior, i.e., $\rho(T, B) = \rho_0 \exp(-U_{act}/kT)$. In the linear temperature range, the extracted activation energy is then $U_{act}(T, B) = U_0(B)[1 - T/T_c]$. For a 3D vortex loops model,^{31,33} the expression of the activation energy is $U_{loop}(T, B) = [\alpha \phi_0^{5/2}/4\pi\mu_0\lambda_{ab}^2(T)\gamma\sqrt{B}]\sqrt{\ln(d\gamma/\xi_{ab})} = U_0(B)[1 - T/T_c]$ where

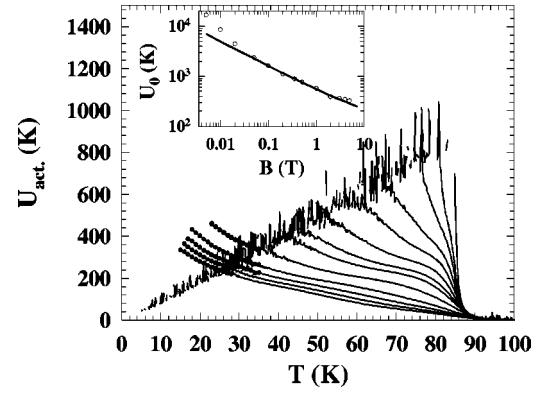


FIG. 5. The temperature dependence of the activation energy for various magnetic field applied parallel to the c -axis direction. The magnetic field is to $B=0, 0.01, 0.02, 0.05, 0.1, 0.2, 0.35, 0.5, 1, 2, 3, 4, 5$ T. The solid lines and the closed circles represent the activation energy obtained by resistivity and ac susceptibility measurements, respectively (see text). The magnetic field dependence of the activation energy is shown in the inset where the solid line corresponds to a $B^{-1/2}$ dependence.

$$U_0(B) = \frac{\alpha \phi_0^{5/2} \sqrt{\ln\left(\frac{d\gamma}{\xi_{ab}}\right)}}{4\pi\mu_0\lambda_{ab}^2(0)\gamma} \frac{1}{\sqrt{B}}.$$

This expression is only valid for the highly anisotropic compound. Here, α is the fitting parameter which should be of order of unity and describes the exact shape of the vortex loop, μ_0 is the permeability of the vacuum, λ_{ab} is the in-plane London penetration depth, ξ_{ab} is the in-plane coherence length. In this model, the activation energy represents the energy required for the creation of a vortex loop allowing a flux line to move from the initial position to a neighboring lacunar site. From the in-plane resistivity curves, we extract the activation energy $U_{act}(T, B)$ as shown by the thin solid line in the Fig. 5. The magnetic field dependence of $U_{act}(T, B)$, and named $U_0(B)$, is deduced from the thermally activated region of $U_{act}(T, B)$ curves. We have plotted the field dependence of U_0 in the inset of the Fig. 5 where the solid line corresponds to the fit of the above expression. From the fit expression and taking the following parameters: $\gamma=100$, $\lambda_{ab}(0)=2000 \text{ \AA}$, $d=12.5 \text{ \AA}$, $\xi_{ab}(0)=20 \text{ \AA}$, we found a very reasonable value of the fitting parameter $\alpha=1.2$. Consequently, the low-temperature part of the in-plane resistivity is correctly described by a 3D loop vortex phase. Let us notice that for $B < 1$ T, the high-temperature limit of the 3D thermally activated behavior corresponds perfectly with the low-temperature limit of the 2D model proposed by Koshelev.¹⁸ For $B > 1$ T, a small temperature range is common to the two models suggesting that the decoupling crossover broaden with the magnetic field. In Fig. 7, this region is illustrated by a gray area. On this figure, we have also plotted the second peak line $B_{sp}(T)$ because it has been observed that the melting line merge to $B_{sp}(T)$.^{35–39} According to this figure, we observe that the melting line and the ob-

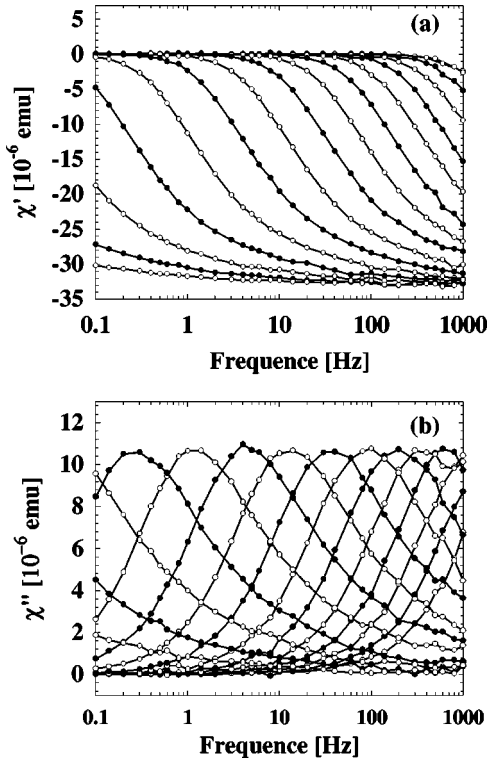


FIG. 6. Frequency dependence of the real (a) and imaginary (b) part of susceptibility for $B=2$ T and for temperature varying between $T=18$ and $T=32$ K with an increment of 1 K (from left to right).

tained experimental line are different, suggesting that the common line of the two above models, experimentally obtained, represents a decoupling crossover inside the liquid phase. This is consistent with Baziljevich *et al.*³⁴ who shown, in Pb-doped Bi-2212 single crystal, that the second peak line was not due to a 3D-2D decoupling.

In order to verify the validity of our resistivity measurements of ρ_{ab} , we have performed ac susceptibility measurements. With this method, only the in plane component of the resistivity is involved.⁴⁰ In order to restrict the measurement to linear regime, we only considered field above $B=1$ T where J_c is negligible. In Fig. 6, we have plotted the frequency dependence of the real χ' [Fig. 6(a)] and imaginary χ'' [Fig. 6(b)] part of the susceptibility for $B=2$ T and for various temperatures between $T=18$ and $T=32$ K. At the maximum of χ'' , the characteristic time of the vortex response is inversely proportional to the frequency (skin effect), i.e., $\tau \approx f_{\max}^{-1}$.⁴⁰ The relation between this characteristic time and the resistivity is given by $\tau = 0.1815(c\mu_0\sqrt{ab}/\pi/\rho)$ where a , b , and c are the dimen-

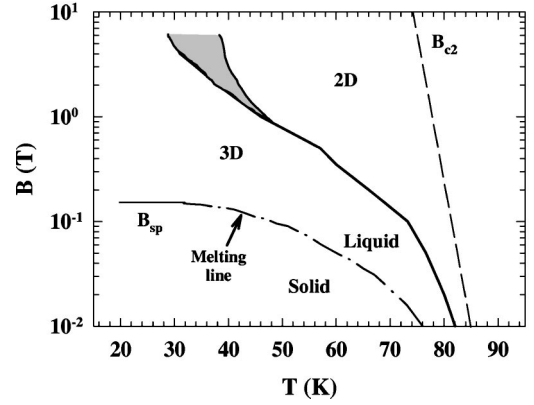


FIG. 7. The (B, T) phase diagram. The solid line represents the decoupling crossover. The dashed line is the upper magnetic field B_{c2} . The gray area corresponds to the range of temperature where the two models described in the text are both valid. The second peak line is represented by B_{sp} and merge to the melting line (dash-dotted line) which is here only a guide for the eye since it is not observed in this crystal.

sions of the sample. Consequently, at the maximum of χ'' , the frequency is proportional to the resistivity and, from the ac susceptibility measurements, we can extract the temperature dependence of the in plane resistivity.⁴¹ The obtained results are plotted in Fig. 5. First, the data obtained by ac susceptibility measurements merge perfectly with those obtained by resistivity ones, confirming the validity of our measurements. For lower temperatures, the temperature dependence of the activation energy deviates from the linearity. Though this remark can be of first importance to understand the low temperature behavior of the vortices, it is out of the scope of the present paper which deals mainly with the 3D to 2D behavior.

In Fig. 7, we have reported the (B, T) phase diagram. In the high magnetic field/high temperature range, i.e., above the solid line, the dissipation is due to a small amount of pancake vortices. In this region, the 2D Koshelev's model is valid. Below this solid line, the vortices present a tridimensional character and the dissipation is due to the movement of 3D vortex loops vortex. Therefore, the solid line represents the crossover from a 3D vortex loops liquid to a 2D decoupled pancake phase.

In conclusion, we have measured, on the same single crystal, both the in-plane and the out-of-plane resistivities. From these data, we have identified a crossover line characterized by the temperature drop (shoulder) of the in-plane resistivity. This line represents the decoupling from a 3D vortex loops liquid state to a 2D decoupled pancake phase.

¹M. Charalambous, J. Chaussy, and P. Lejay, Phys. Rev. B **45**, 5091 (1992).

²H. Safar, P.L. Gammel, D.A. Huse, D.J. Bishop, J.P. Rice, and D.M. Ginsberg, Phys. Rev. Lett. **69**, 824 (1992).

³D.T. Fuchs, E. Zeldov, D. Majer, R.A. Doyle, T. Tamegai, S.

Ooi, and M. Konczykowski, Phys. Rev. B **54**, R796 (1996).

⁴D.T. Fuchs, R.A. Doyle, E. Zeldov, D. Majer, W.S. Seow, R.J. Drost, T. Tamegai, S. Ooi, M. Konczykowski, and P.H. Kes, Phys. Rev. B **55**, R6156 (1997); Physica C **282**, 2023 (1997).

- ⁵D. Lopez, E.F. Righi, G. Nieva, and F. de la Cruz, *Phys. Rev. Lett.* **76**, 4034 (1996).
- ⁶W.K. Kwok, S. Fleshler, U. Welp, V.M. Vinokur, J. Downey, G.W. Crabtree, and M.M. Miller, *Phys. Rev. Lett.* **69**, 3370 (1992).
- ⁷W.K. Kwok, J. Fendrich, U. Welp, S. Fleshler, J. Downey, and G.W. Crabtree, *Phys. Rev. Lett.* **72**, 1088 (1994).
- ⁸J.A. Fendrich, W.K. Kwok, J. Giapintzakis, C.J. Van der Beek, V.M. Vinokur, S. Flesher, U. Welp, H.K. Viswanathan, and G.W. Crabtree, *Phys. Rev. Lett.* **74**, 1210 (1995).
- ⁹T. Sasagawa, Y. Togawa, J. Shimoyama, A. Kapitulnik, K. Kitazawa, and K. Kishio, *Phys. Rev. B* **61**, 1610 (2000).
- ¹⁰G. Blatter, M.V. Feigel'man, V.M. Geshkenbeim, A.I. Larkin, and V.M. Vinokur, *Rev. Mod. Phys.* **66**, 1125 (1994).
- ¹¹T. Sasagawa, K. Kishio, Y. Togawa, J. Shimoyama, and K. Kitazawa, *Phys. Rev. Lett.* **80**, 4297 (1998).
- ¹²T.T.M. Palstra, B. Batlogg, L.F. Schneemeyer, and J.V. Waszczak, *Phys. Rev. Lett.* **61**, 1662 (1988).
- ¹³T.T.M. Palstra, B. Batlogg, L.F. Schneemeyer, R.B. Van Dover, and J.V. Waszczak, *Phys. Rev. B* **38**, 5102 (1988).
- ¹⁴T.T.M. Palstra, B. Batlogg, R.B. Van Dover, L.F. Schneemeyer, and J.V. Waszczak, *Phys. Rev. B* **41**, 6621 (1990).
- ¹⁵D.H. Kim, K.E. Gray, R.T. Kampwirth, and D.M. Mc Kay, *Phys. Rev. B* **42**, 6249 (1990).
- ¹⁶J.T. Kucera, T.P. Orlando, G. Virshup, and J.N. Eckstein, *Phys. Rev. B* **46**, 11 004 (1992).
- ¹⁷L.I. Glazman and A.E. Koshelev, *Phys. Rev. B* **43**, 2835 (1991).
- ¹⁸A.E. Koshelev, *Phys. Rev. Lett.* **76**, 1340 (1996).
- ¹⁹R. Busch, G. Ries, H. Werthner, G. Kreiselmeyer, and G. Saemann-Ischenko, *Phys. Rev. Lett.* **69**, 522 (1992).
- ²⁰T. Aouaroun, V. Hardy, C. Goupil, F. Warmont, G. Villard, and Ch. Simon, *Supercond. Sci. Technol.* **10**, 572 (1997).
- ²¹G. Villard, D. Pelloquin, A. Maignan, and A. Wahl, *Physica C* **278**, 11 (1997).
- ²²A. Ruyter, Ch. Simon, V. Hardy, M. Hervieu, and A. Maignan, *Physica C* **225**, 235 (1994).
- ²³V. Hardy, A. Maignan, C. Martin, F. Warmont, and J. Provost, *Phys. Rev. B* **56**, 130 (1997).
- ²⁴D.T. Fuchs, R.A. Doyle, E. Zeldov, S.F.W.R. Rycroft, T. Tamegai, S. Ooi, M.L. Rappaport, and Y. Myasoedov, *Phys. Rev. Lett.* **81**, 3944 (1998).
- ²⁵Y.M. Wan, S.E. Hebboul, D.C. Harris, and J.C. Garland, *Phys. Rev. Lett.* **71**, 157 (1993).
- ²⁶Y.M. Wan, S.E. Hebboul, and J.C. Garland, *Phys. Rev. Lett.* **72**, 3867 (1993).
- ²⁷X.H. Chen, M. Yu, K.Q. Ruan, S.Y. Li, Z. Gui, G.C. Zhang, and L.Z. Cao, *Phys. Rev. B* **58**, 14 219 (1998).
- ²⁸Y.F. Yan, P. Matl, J.M. Harris, and N.P. Ong, *Phys. Rev. B* **52**, R751 (1995).
- ²⁹M. Chung, H. Chang, Y.J. Doh, and H. Lee, *Solid State Commun.* **105**, 25 (1998).
- ³⁰Y. Sun, G.Y. Xu, J. Du, Y. Zhou, R. Zeng, X. Fu, P. Hua, and Y. Zhang, *Phys. Rev. B* **54**, 1382 (1996).
- ³¹F. Warmont, Ch. Goupil, V. Hardy, and Ch. Simon, *Phys. Rev. B* **58**, 132 (1998).
- ³²X. Xiaojun, F. Lan, W. Liangbin, Z. Yuheng, F. Jun, C. Xiaowen, and S. Hisashi, *Phys. Rev. B* **59**, 608 (1999).
- ³³Ch. Goupil, Ph.D. thesis, Université de Caen, 1997.
- ³⁴M. Baziljevich, D. Giller, M. McElfresh, Y. Abulafia, Y. Radzyner, J. Schneck, T.H. Johansen, and Y. Yeshurun, *Phys. Rev. B* **62**, 4058 (2000).
- ³⁵T. Hanaguri, T. Tsuboi, A. Maeda, T. Nishizaki, N. Kobayashi, Y. Kotaka, J.I. Shimoyama, and K. Kishio, *Physica C* **256**, 111 (1996).
- ³⁶B. Khaykovich, E. Zeldov, D. Majer, T.W. Li, P.H. Kes, and M. Konczykowski, *Phys. Rev. Lett.* **76**, 2555 (1996).
- ³⁷P.H. Kes, H. Pastoriza, T.W. Li, R. Cubitt, E.M. Forgan, S.L. Lee, M. Konczykowski, B. Khaykovich, D. Majer, D.T. Fuchs, and E. Zeldov, *J. Phys. I* **6**, 2327 (1996).
- ³⁸D.T. Fuchs, E. Zeldov, T. Tamegai, S. Ooi, M. Rappaport, and H. Shtrikman, *Phys. Rev. Lett.* **80**, 4971 (1998).
- ³⁹S. Ooi, T. Shibauchi, and T. Tamegai, *Physica C* **302**, 339 (1998).
- ⁴⁰T. Aouaroun and Ch. Simon, *Phys. Rev. B* **58**, 11 692 (1998).
- ⁴¹C. Goupil, A. Ruyter, J. Provost, T. Aouaroun, and C. Simon, *J. Phys. III* **5**, 1481 (1995).